# Static characteristics of pulsed actuator with combined plunger

Ivo Doležel
Czech Technical University
166 27 Praha 6, Technicka 2, e-mail: dolezel@fel.cvut.cz)

David Pánek, Bohuš Ulrych
University of West Bohemia
306 14 Plzen, Univerzitni 26, e-mail: panek50@kte.zcu.cz, ulrych@kte.zcu.cz)

A novel type of pulsed electromagnetic actuator is presented and modelled. Its plunger consists of two cylindrical parts made of classical magnetic material and permanent magnet, respectively. Its motion is controlled by short current pulses of the prescribed amplitude. The paper starts with the definition of the technical problem and formulation of its mathematical model. This model is then solved numerically and the whole methodology is illustrated by a typical example, whose results are discussed.

## 1. Introduction

Electromagnetic actuators (see, for example [1], [2] and [3]) are widely used in numerous industrial, transport, robotic, and other systems. Mostly they are used for converting electric energy into mechanical forces and torques.

The basic disadvantage of classical electromagnetic actuators is the fact that they require delivery of electric current during full time of their active operation. A longer time of operation, however, may result in a high consumption of electric energy and, consequently, in undesirable overheating of the system.

This disadvantage can be suppressed by the use of combined electromagnetic actuators, where the transient switching-on and switching-off processes are controlled by short electric pulses, but the steady-state switch-on (or even switch-off) regime is only realized by a permanent magnet, i.e., without delivery of any external energy to the system. In this way we also avoid consequent overheating.

One actuator of this type is analyzed in this paper. First, its arrangement is described together with the material properties of its individual structural parts. Then, the corresponding mathematical and computer models are given and explained. Their solution (carried out by a combination of the finite element method allows predicting its operation properties. The crucial point of the paper is the presentation of the static characteristics obtained for one particular version of such an actuator. The most important results are discussed.

## 2. Formulation of the technical problem

The actuator is depicted in Fig. 1. Its left part shows the state of the device before the process of its switching on, the right one a similar state before the process of its switching off.

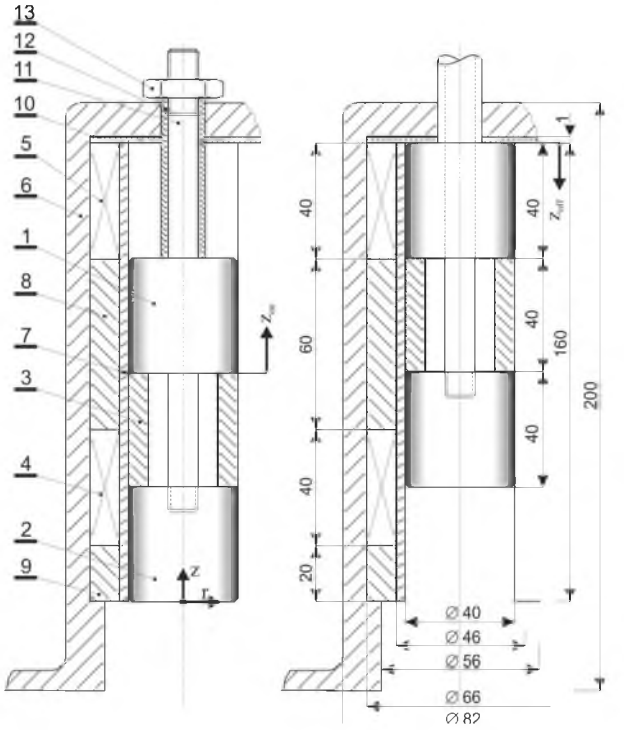


Fig. 1. Arrangement of the considered actuator, dimensions given in millimeters (switch-off left, switch-on right): **1**–permanent magnet, **2**–ferromagnetic element, **3**–nonmagnetic distance shell, **4**–coil controlling element **2**, **5**–coil controlling magnet **1**, **6**–ferromagnetic shell of the actuator with lid, **7**–nonmagnetic slotted leading shell, **8**, **9**–dilatation spacers, **10**–nonmagnetic distance spacer, **11**–nonmagnetic draw-bar, **12**–nonmagnetic pipe, **13**–connecting nut

The plunger consists of a permanent magnet **1** and ferromagnetic element **2**. These two parts are connected mechanically by a nonmagnetic drag-bar **11** and equipped with elements **3** and **12**. The plunger is placed in the ferromagnetic shell **6** and its axial movement is fixed by another nonmagnetic leading shell **7**. The shells **6** and **7** contain axial slots eliminating the hydraulic resistances during the movement of the plunger.

The movements of the plunger in the direction $z_{\mathrm{on}}$ (transition from the switch-off regime into the switch-on regime) or $z_{\mathrm{off}}$ (vice versa) are controlled by

magnetic fields generated by coils $C_1 \approx \mathbf{4}$ and $C_2 \approx \mathbf{5}$ carrying pulsed currents $I_{\text{on}}$ (on) or $I_{\text{off}}$ (off). The above coils are fixed by nonmagnetic distance spacers **8**, **9** and **10**. The drag-bar **11** transfers the generated force out of the actuator. Finally, the nut **13** on it defines the starting position of the plunger.

The operation regimes of the actuator are two: on and off. They are realized in the manners described in the following paragraphs.

- When switching on the switched-off actuator (see Fig. 1, left part), a current pulse $I_{\text{on}}$ is delivered to field coil $C_1 \approx \mathbf{4}$. Now the ferromagnetic part **2** of the plunger starts to be pulled into it by force $\boldsymbol{F}_{\text{m2on}}$. The pulsed current $I_{\text{on}}$ should be switched off (using, for example, a phototransistor) approximately at the moment when the ferromagnetic part is completely in the coil). As the connected permanent magnet **1** approaches the ferromagnetic lid of the shell **6**, it is attracted to it and, finally, the plunger gets into the position depicted in Fig. 1, right part.
- When switching off the switched-on actuator, we have to deliver an appropriately oriented pulse $I_{\text{off}}$ to the field coil $C_2 \approx \mathbf{5}$ in order to demagnetize the permanent magnet **1**, which leads to a strong decrease of the force attracting it to the lid. At the same time, the same pulsed current $I_{\text{off}}$ is also delivered to the field coil $C_1 \approx \mathbf{4}$. The ferromagnetic part of the plunger is again pulled into this field coil (now by force $\boldsymbol{F}_{\text{m2off}}$). In this way, the actuator is switched off.

## 3. Mathematical model of the problem

The general equation describing the distribution of electromagnetic field in the actuator reads [4]

$$\operatorname{curl}\left(\frac{1}{\mu}\operatorname{curl}\boldsymbol{A}-\boldsymbol{H}_{\text{c}}\right)=\boldsymbol{J}, \tag{1}$$

where $\boldsymbol{A}$ denotes the magnetic vector potential, symbol $\mu$ stands for the magnetic permeability, $\boldsymbol{J}$ is the field current density (only in the field coils), and $\boldsymbol{H}_{\text{c}}$ denotes the coercive force (only in the domain of permanent magnets). In the cylindrical coordinates both field current density $\boldsymbol{J}$ and magnetic vector potential $\boldsymbol{A}$ have only one nonzero component $J_\varphi$ and $A_\varphi$ in the circumferential direction.

The boundary conditions along the axis of the arrangement and along the boundary of the investigated domain (axial cut of the device) are of the Dirichlet type ($A_\varphi = 0$). This artificial boundary may be (with a negligible error)

represented by the external surface of the actuator.

The general vector of the magnetic force $\boldsymbol{F}_{\mathrm{m}}$ acting on ferromagnetic elements of the actuator is given [5] by the integral

$$\boldsymbol{F}_{\mathrm{m}} = \frac{1}{2}\oint_S \left(\boldsymbol{H}\left(\boldsymbol{n}\cdot\boldsymbol{B}\right) + \boldsymbol{B}\left(\boldsymbol{n}\cdot\boldsymbol{H}\right) - \boldsymbol{n}\left(\boldsymbol{H}\cdot\boldsymbol{B}\right)\right)\mathrm{d}S\,, \tag{2}$$

where $\boldsymbol{B}$ and $\boldsymbol{H}$ are the field vector, $\boldsymbol{n}$ denotes the unit outward normal and the integration is carried out along the whole surface $S$ of both ferromagnetic parts and the permanent magnet. The force $\boldsymbol{F}_{\mathrm{m}}$ is formed by the following partial forces (all of them are supposed to have only one component in the axial direction):

- $F_{\mathrm{m1}}$ - force acting (see Fig. 1) on the permanent magnet **1** in the direction $\boldsymbol{z}_{\mathrm{on}}$ during both processes of switching on and switching off. The permanent magnet is always attracted to the flat lid of the ferromagnetic shell **6**.
- $F_{\mathrm{m2on}}$ - force acting on the ferromagnetic element **2** in the direction $\boldsymbol{z}_{\mathrm{on}}$ (see Fig. 1) in the process of switching on (the element is pulled into the field coil $\mathrm{C}_1 \approx \mathbf{4}$ regardless the orientation of the pulsed current $I_{\mathrm{on}}$ provided it is switched off in time).
- $F_{\mathrm{m2off}}$ - force acting on the ferromagnetic element **2** in the direction $\boldsymbol{z}_{\mathrm{off}}$ (see Fig. 1) in the process of switching off (the element is pulled into the field coil $\mathrm{C}_1 \approx \mathbf{4}$ regardless the orientation of the pulsed current $I_{\mathrm{off}}$ provided it is switched off in time).

## 4. Computer model

The mathematical model of the actuator (equations (1) and (2) was solved as a nonlinear axisymmetric 2D problem in the cylindrical coordinates $(r, z)$ using the FEM-based code QuickField 6 [6]. The goal of the computations was to obtain (as fast as possible) all necessary information, particularly the force conditions in the actuator in both steady-state operation regimes that will be used for the construction of its static characteristics..

Carefully was checked the convergence of the solution on the density of the discretization mesh. Some results were checked by our own fully adaptive code Agros2d [7] based on a fully adaptive higher-order finite element method.

## 5. Illustrative example

Analyzed was the actuator depicted in Fig. 1. Its geometry is known and list of the physical properties of materials used for its construction is given in Tab. 1. All these materials are available in practically every laboratory. The only exception is perhaps the element **1**, manufactured of a ferrite permanent magnet Koerox 420

[8]. The magnet exhibits a very low electric conductivity in order to avoid generation of eddy currents in it during the processes of switching on and switching off, when the field coils carry currents $I_{\text{on}}$ and $I_{\text{off}}$, respectively.

Table 1. Materials used for the actuator (see Fig. 1)

| Item | Element | Material | $\mu_r$ (-) |
|---|---|---|---|
| **1** | permanent magnet | Koerox 420 [4] | Fig. 2 |
| **2** | ferromagnetic core | steel 12 040 | Fig. 3 |
| **3** | distance shell | nylon | 1 |
| **4** | coil $C_1$ | Cu wire, Ø 1 mm | 1 |
| **5** | coil $C_2$ | Cu wire, Ø 1 mm | 1 |
| **6** | shell | steel 12 040 | Fig. 2 |
| **7** | leading shell | nylon | 1 |
| **8, 9** | dilatation spacers | brass | 1 |
| **10** | distance spacer | brass | 1 |
| **11** | connecting draw-bar | brass | 1 |
| **12** | distance pipe | brass | 1 |
| **13** | connecting nut | brass | 1 |

Its demagnetization characteristic is depicted in Fig. 2. During the repeated demagnetization and magnetization of the permanent magnet it is only possible to make use of the straight part of its demagnetization characteristic, because only in this case the corresponding secondary hysteresis loops transform into straight lines, i.e., the magnet is not deteriorated energetically. The acceptable working interval of magnet Koerock 420 ranges (see Fig. 2, the dashed line) within the interval $B \in (0.178,\ 0.678)\,\text{T}$.

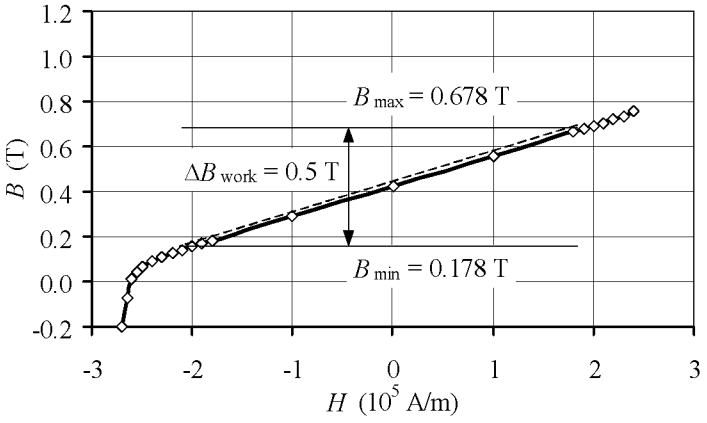


Fig. 2. Demagnetization curve and operation interval of magnet Koerock 420 [8]

The ferromagnetic shell **6** of the actuator and ferromagnetic element **2** of the plunger are manufactured of material with the lowest possible magnetic resistance that must also be cheap and easily machinable. We selected a low-alloyed carbon steel CSN 12 040 whose magnetization characteristic is shown in Fig. 3.

The computer model described in the previous section allowed obtaining all required results, mainly of the quantitative character. Nevertheless, first we checked the convergence of the solution on the density of the discretization mesh. The relevant data providing a good idea about the accuracy of the solution are listed in Tab. 2.

One of the main results is that in the process of switching off both current pulses $I_{\mathrm{off}}(\mathrm{C}_1)$ and $I_{\mathrm{off}}(\mathrm{C}_2)$ must be oriented equally, and must appropriately demagnetize the permanent magnet **1**. Other results follow.

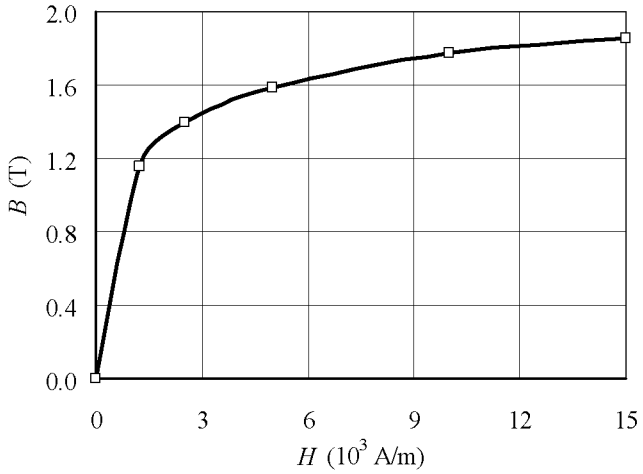


Fig. 3. Nonlinear magnetization characteristic of steel CSN 12 040

Table 2. Convergence of the results ( $I_{\mathrm{on}} = 0$, $z_{\mathrm{on}} = 40$ mm)

| Parameters of mesh | | Results | |
|---|---|---|---|
| Number of nodes (-) | Spacing (mm) | $B_{\mathrm{l,avrg}}$ (T) | $F_{\mathrm{m1on}}$ (N) |
| 9254 | 1.0/2.0/10.0 | 0.357 | 52.067 |
| 35839 | 0.5/1.0/5.0 | 0.357 | 53.731 |
| 81489 | 0.25/0.5/2.5 | 0.357 | 54.887 |
| 251147 | 0.125/0.25/1.25 | 0.357 | 55.227 |

Figure 4 shows the influence of the demagnetization current $I_{\mathrm{off}}(\mathrm{C}_2)$ on the situation in the permanent magnet **1**. As the average value $B_{\mathrm{l,avrg}}$ of magnetic flux density in it decreases, the force $F_{\mathrm{m1}}$ acting in the direction $z_{\mathrm{on}}$ also decreases.

But as we are limited by the straight part of the demagnetization characteristic (see Fig. 2), the maximum acceptable value of the demagnetization current $I_{\mathrm{off}}(\mathrm{C}_2) = -16\,\mathrm{A}$ for $z_{\mathrm{off}} = 0\,\mathrm{mm}$. For this value $B_{\mathrm{l,avrg}} = 0.183\,\mathrm{T}$ and $F_{\mathrm{m1}} \approx 20\,\mathrm{N}$. And this force must be exceeded by the force $F_{\mathrm{m2off}}$, by which the ferromagnetic element **2** is (using the same current $I_{\mathrm{off}}(\mathrm{C}_1) = -16\,\mathrm{A}$) pulled into field coil $\mathrm{C}_1$.

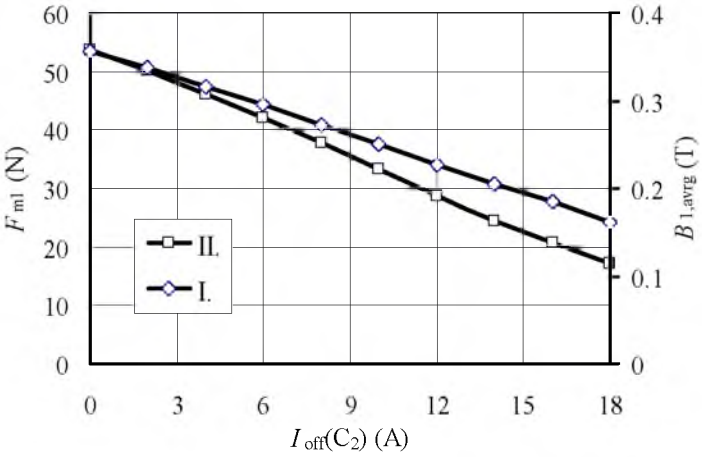


Fig. 4. Dependence of two important characteristics on current $I_{\mathrm{off}}(\mathrm{C}_2)$ : I– $F_{\mathrm{m1}}$ , II– $B_{\mathrm{l,avrg}}$

Figure 5 shows the static characteristic of the permanent magnet **1** in the switching-on regime, i.e., the dependence of force $F_{\mathrm{m1}}$ acting on the magnet on its position $z_{\mathrm{on}}$ in the actuator ($z_{\mathrm{on}} \in \langle 0,\ 40 \rangle\,\mathrm{mm}$). Another depicted curve is the corresponding average magnetic flux density $B_{\mathrm{l,avrg}}$ in the magnet. It is obvious that at the beginning of the process the force $F_{\mathrm{m1}}$ is very low and starts increasing only at a half of its way to the ferromagnetic lid. There it reaches its maximum value $F_{\mathrm{m1,max}} \approx 54\,\mathrm{N}$. Thus, this is the maximum attractive force that can be generated without external source of energy. On the other hand, the average value $B_{\mathrm{l,avrg}}$ of magnetic flux density in permanent magnet **1** is practically independent of the position $z_{\mathrm{on}}$; it slightly increases only when the magnet approaches the lid. This is caused by a mild homogenization of magnetic field in this position – a part of force lines entry practically perpendicularly the lid.

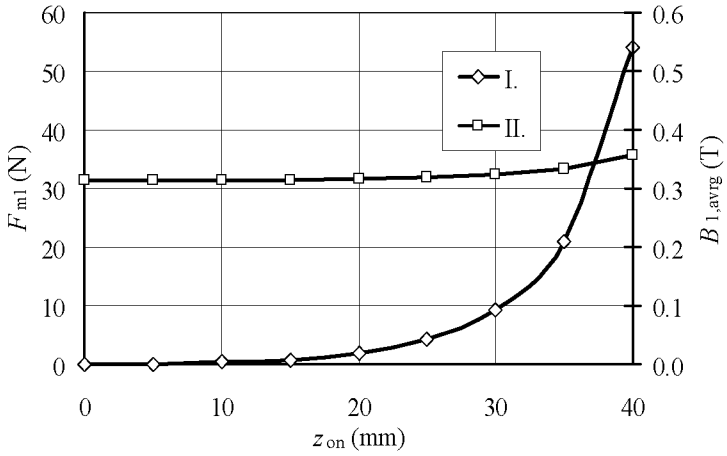


Fig. 5. Static characteristic of the permanent magnet **1** in the switching-on regime $I_{on}(C_1) = I_{on}(C_2) = 0$ (I– $F_{m1}$ , II– $B_{1,avrg}$ )

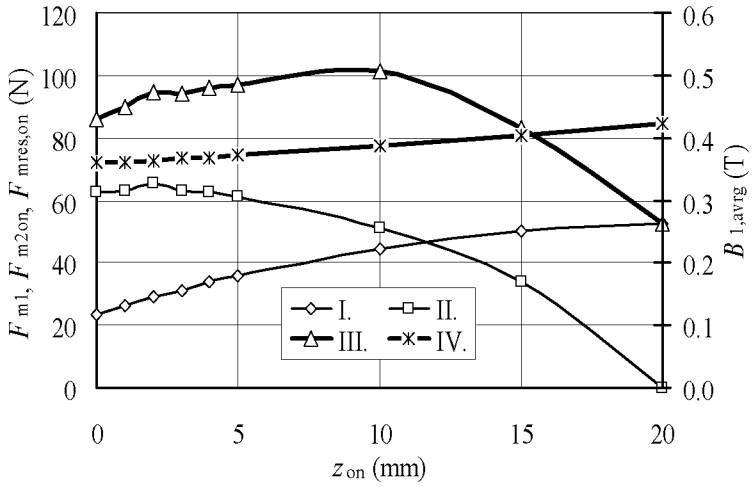


Fig. 6. Static characteristic of the whole actuator in the switching-on regime $I_{on}(C_1) = I_{on}(C_2) = 16$ A (I– $F_{m1}$ , II– $F_{m2on}$ , III– $F_{mres\ on}$ , IV– $B_{1,avrg}$ )

Figure 6 depicts the resultant static characteristic of the whole actuator within the range $z_{on} \in \langle 0, 20 \rangle$ mm. This range corresponds to the position of ferromagnetic part **2** of the plunger in field coil $C_1 \approx \mathbf{4}$, where we obtain $F_{mres\ on} = F_{m1} + F_{m2on}$ (both forces $F_{m1}$ and $F_{m2on}$ being dependent on $z_{on}$ and pulsed current $I_{on}$ . In the remaining interval $z_{on} \in \langle 20, 40 \rangle$ mm there holds

$F_{\text{mres on}} = F_{\text{m1}}$ where $F_{\text{m1}}$ only depends on $z_{\text{on}}$ – see Fig. 5. Here the pulsed current $I_{\text{on}}$ has to be switched off, otherwise the ferromagnetic part **2** would be pulled again into the coil $\text{C}_1 \approx \mathbf{4}$. The local maximum in line II visible near the point $z_{\text{on}} = 2\,\text{mm}$ shows the place of the highest force $F_{\text{m2on}}$ acting on the ferromagnetic part **2** of the plunger.

Finally, Fig. 7 contains the resultant switch-off characteristic of the whole device, again within the range $z_{\text{off}} \in \langle 0, 20 \rangle\,\text{mm}$ corresponding to the position of ferromagnetic part **2** of the plunger just inside the field coil $\text{C}_1$. Here the resultant force is $F_{\text{mres off}} = F_{\text{m1}} + F_{\text{m2off}}$. Now both forces on the right-hand side depend on $z_{\text{off}}$ and pulsed current $I_{\text{off}}$. In the remaining interval $z_{\text{off}} \in \langle 20, 40 \rangle\,\text{mm}$ there holds $F_{\text{mres off}} = F_{\text{m1}}$ where $F_{\text{m1}}$ only depends on $z_{\text{off}} = 40 - z_{\text{on}}$. Here the pulsed current $I_{\text{off}}$ has to be switched off. Further movement of the plunger is realized by inertia or by means of a draw spring (which, however, is not present in Fig. 1).

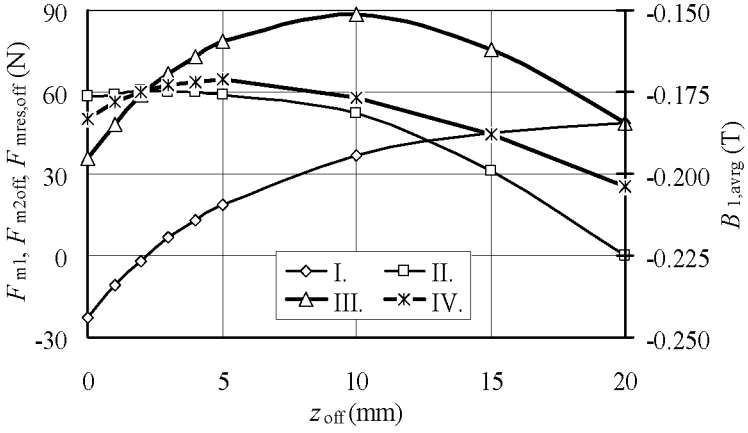


Fig. 7. Static characteristic of the whole actuator in the switching-off regime $I_{\text{off}}(\text{C}_1) = I_{\text{off}}(\text{C}_2) = -16$ A (I– $F_{\text{m1}}$, II– $F_{\text{m2off}}$, III– $F_{\text{mres off}}$, IV– $B_{\text{1,avrg}}$)

At this place, it is necessary to remark that the permanent magnet is influenced by forces produced by both ferromagnetic material and external magnetic field in its neighbourhoods. That is why the force $F_{\text{m1}}$ changes its sign within the interval $z_{\text{off}} \in \langle 0, 20 \rangle\,\text{mm}$, see line I in Fig. 7. At the beginning, for small values of $z_{\text{off}}$ the permanent magnet **1** is attracted to the lid of the ferromagnetic shell **6**. With respect to the direction of vector $\boldsymbol{z}_{\text{off}}$ (see the right part of Fig. 1) the force $F_{\text{m1}}$ is

oriented negatively. But for higher values of $z_{\mathrm{off}}$ the permanent magnet **1** is more strongly attracted to the field generated by the field coil $\mathrm{C}_1 \approx \mathbf{4}$ that carries pulsed current $I_{\mathrm{off}}$. Now, the force $F_{\mathrm{m1}}$ is positive with respect to vector $\boldsymbol{z}_{\mathrm{off}}$. At the moment when the permanent magnet reaches $z_{\mathrm{off}} = 20$ mm and the pulsed current $I_{\mathrm{off}}$ vanishes, the force $F_{\mathrm{m1}}$ drops from the value about $50\,\mathrm{N}$ (Fig. 7, line I) to value $-2\,\mathrm{N}$ oriented against $\boldsymbol{z}_{\mathrm{off}}$, see Fig. 5. This means that the permanent magnet is again attracted to the lid of ferromagnetic shell **6**, but due to a longer distance this force is already small. In case of still growing $z_{\mathrm{off}} = 40 - z_{\mathrm{on}}$, the force $F_{\mathrm{m1}} \to 0$.

## 6. Conclusion

The proposed actuator is able to realize the basic steady-states (switch-on and switch-off regimes) without any delivery of external energy. The transients (processes of switching on and switching off) are controlled by means of short external pulsed currents. These can be obtained, for example, using appropriate electric circuits containing sufficiently strong capacitors. Due to these advantages, the actuator could be very prospective in a number of technical applications.

Next work will be focused on modelling of the dynamic characteristic of the device and experimental verification of the results.

### Acknowledgment

*The financial support of the Grant Agency of the Czech Republic (project No. 102/09/1305), Research Plan MSM 6840770017 is gratefully acknowledged.*

### References

[1] H. Janocha, Actuators, Basics & Applications, Springer, New York, 2004.
[2] J. R. Brauer, Magnetic Actuators and Sensors, Wiley, New York, 2006.
[3] I. J. Bush-Vishniac, Electromagnetic Sensors and Actuators, Springer, Berlin, 1998.
4] E. P. Furlani, Permanent Magnet and Electromechanical Devices, Academic Press, New York, 2001.
[5] M. Kuczmann, A. Iványi, The Finite Element Method in Magnetics, Akademiai Kiadó, Budapest, 2008.
[6] QuickField, www.quickfield.com.
[7] Agros2d, http://www.agros2d.org/.
[8] Koerox magnets, http://www.kolektor.si/resources/files/ doc/magneti/KoeroxI.pdf.